Aggregation Efficiency of Activated Normal or Fixed Platelets in a Simple Shear Field: Effect of Shear and Fibrinogen Occupancy

Zheming Xia and Mony M. Frojmovic
Department of Physiology, McGill University, Montreal, Quebec H3G 1Y6, Canada

ABSTRACT Shear rate can affect protein adsorption and platelet aggregation by regulating both the collision frequency and the capture efficiency (α). These effects were evaluated in well defined shear field in a micro-couette for shear rate G = 10 – 1000 s^{-1}. The rate of protein binding was independent of G, shown for adsorption of albumin to latex beads and PAC1 to activated platelets. The initial aggregation rate for ADP-activated platelets in citrated platelet-rich plasma followed second order kinetics at the initial platelet concentrations between 20,000 and 60,000/μl. α values, which dropped nearly fivefold for a 10-fold increase in G, were approximately proportional to G^{-1}, contrary to a minor drop predicted by the theory that includes protein cross-bridging. Varying ADP concentration did not change α of maximally activated platelet subpopulations, suggesting that aggregation between unactivated and activated platelets is negligible. Directly blocking the unoccupied but activated GPIIb-IIIa receptors without affecting pre-bound Fg on "RGD"-activated, fixed platelets (AFP) by GRGDSP or Ro 43–5054 eliminated aggregation, suggesting that cross-bridging of GPIIb-IIIa on adjacent platelets by fibrinogen mediates aggregation. α for AFP remained maximal (~0.24) over 25–75% Fg occupancy, otherwise decreasing rapidly, with a half-maximum occurring at around 2% occupancy, suggesting that very few bound Fg were required to cause significant aggregation.

INTRODUCTION

There are both biochemical and physical determinants of cell aggregation. Thus, it is widely recognized that fibrinogen occupancy of the expressed GPIIb-IIIa receptors on the activated platelet membrane is a prerequisite for platelet aggregation (Marguerie et al., 1980; Niewiarowski et al., 1983; Peerschke, 1985; Plow and Ginsberg, 1989). In addition, the rate and extent of the aggregation in flowing suspensions in vitro and in the circulation in vivo are governed by shear. Shear stress, whose time average values in the normal blood circulation range from approximately 1 to 20 dyn/cm^2 (Milnor, 1982), can have multiple effects on aggregation by regulating: (i) the collision frequency between the platelets in the suspension; (ii) the efficiency of platelet adhesion, which generally decreases with increasing shear stress; (iii) the kinetics of Fg binding on activated GPIIb-IIIa when the shear-driven collision frequency between platelet and fibrinogen exceeds the diffusion driven one; (iv) at moderate shear rate, the release of ADP from dense granules, which is responsible for aggregation (Anderson et al., 1978; Belval et al., 1984); and (v) at higher shear rate, the activation of the GPIb receptor and/or von Willebrand factor (vWF), where vWF is present in plasma, can also be released from α-granules, and which can bind to either GPIb or activated GPIIb-IIIa (Ikeda et al., 1991; Joist et al., 1985; Petersom et al., 1987).

Kinetics of aggregation under varying shear will be dependent on kinetics of fibrinogen binding if the rate of fibrinogen binding is comparable to that of aggregation. Preincubation of platelets with fibrinogen separates fibrinogen binding from aggregation, assuming that the same fibrinogen binding rate can be achieved regardless of the applied shear. However, because fibrinogen binding has generally been studied in nonflowing conditions (Bennett and Gaston, 1979; Warkentin et al., 1990), it is not clear whether and how shear affects its binding rate.

The kinetics of aggregation in flow have largely been studied under stir in aggregometers, where the hydrodynamic conditions cannot be specified (Lumley and Humphrey, 1981; Peerschke and Zucker, 1981). Moreover, the conventional light transmission method of quantifying aggregates was not sufficiently sensitive to detect micro-aggregates composed mainly of doublets and triplets (Pedvis et al., 1988), although the interpretation of turbidimetric measurements has been improved based on light scattering theory (Chang and Robertson, 1976; Hantgan, 1985). Electronic particle counting (Frojmovic et al., 1989; Huang and Hellums, 1993) is a more straightforward and accurate technique to determine aggregation. Platelet aggregation has also been studied under well defined hydrodynamic conditions, for instance, in capillary tubes (Bell and Goldsmith, 1984) where local or average shear rate are known, or in a cone-and-plate viscometer (Belval et al., 1984; Huang and Hellums, 1993; Klose et al., 1975) or couette apparatus (Chang and Robertson, 1976) where shear rates are uniform. Although these well characterized shear fields enable the determination of frequency of collision between platelets,

Received for publication 22 November 1993 and in final form 15 March 1994.

Address reprint requests to Dr. M. M. Frojmovic, Department of Physiology, McGill University, McIntyre Medical Sciences Bldg., 3655 Drummond St., Rm. 1102, Montreal, Quebec H3G 1Y6, Canada. Tel: 514-398-4326; Fax: 514-398-7452; E-mail: mony@medcor.mcgill.ca.

Zheming Xia is a post-doctoral research fellow from Heart and Stroke Foundation of Canada.

0006-3495/94/06/2190/12 $2.00

and consequently, the efficiency of aggregation, the measurement of the effect of shear on efficiency of aggregation has been limited only to relatively low shear rates (<100 s^{-1}) (Bell and Goldsmith, 1984; Chang and Robertson, 1976). No attempts have been made to correlate the efficiency with fibrinogen occupancy on the GPIIb-IIIa receptor on platelets. Determination of capture efficiency has essentially been based on Smolukowski model of two-body collision kinetics, assuming that hydrodynamic drag force on the colliding platelets are balanced by the attractive colloidal forces (e.g., van der Waals forces). This model, although restricted to the early stage of aggregation, has been accepted to describe a wide variety of systems, including latex spheres (Higuchi et al., 1963; Varennes et al., 1988), and hydrosols (Swift and Friedlander, 1964). Recently, more sophisticated models have also been developed (Potanin et al., 1993) in which ligand/receptor interaction and elasticity of platelets were incorporated into an analytical solution of lubrication theory.

This study focuses on effect of shear (100–1000 s^{-1}) and of Fg occupancy on the aggregation efficiency of normal platelets and of preactivated and fixed human platelets (AFP) under simple shear field in a micro-couette. We also report on the kinetics of protein binding onto either latex beads or AFP, both in the presence and absence of shear, using flow cytometry.

MATERIALS AND METHODS

Reagents

The following reagents were used: human fibrinogen (Enzyme Research Laboratories Inc., South Bend, IN); PAC1, a monoclonal antibody (IgM) specific for activated GPIIb-IIIa receptors on stimulated platelets (purchased from University of Pennsylvania, Philadelphia, PA, via Dr. S. Shattil); 9F9, a monoclonal antibody (IgG) having specificity for GPIIb-IIIa bound Fg (Purchased from Dr. Andrei Budzynski, Temple University, Philadelphia, PA); S12, a monoclonal antibody specific to platelet α-granule membrane protein GMP 140 (gift from Dr. Rodger McEver, Oklahoma Medical Research Foundation, Oklahoma city, OK); ZK 36 374, a stable prostacyclin analog (gift from Dr. T. Krais, Schering Co., Berlin, Germany); H-Gly-Arg-Gly-Asp-Ser-Pro-OH peptide (GRGDSP, Calbiochem Corporation, La Jolla, CA); Carboxylated polystyrene latex beads (2.01 μm in diameter; Polysciences, Inc., Warrinton, PA); BSA (Fraction V, Sigma Chemical Co., St. Louis, MO); ADP (Sigma); Ro 43–5054, a nonpeptide analog of GRGDSP (gift from Dr. T. Weller, F. Hoffmann-La Roche Ltd., Basel, Switzerland); Glutaraldehyde (electron microscopy grade; Polysciences Inc.); SurfaSil, siliconizing fluid (Pierce, Rockford, IL); Paraformaldehyde (Fisher Scientific Company, Fairlawn, NJ).

Preparation of platelet suspensions

Platelet-rich plasma

Venous blood was slowly drawn from healthy volunteers via a 19-gauge needle into a 20–40 ml plastic syringe. The blood was immediately transferred to 15 ml polypropylene tubes containing 1/10 volume 3.8% sodium citrate. After mixing by gently inverting the tubes, the blood was centrifuged at room temperature at 150 × g for 15 min. The supernatant platelet rich plasma (PRP), containing from 3 to 6 × 10^5 cells μl^{-1}, was transferred to another polypropylene tube and kept at 37°C under a mixture of 95% air and 5% CO_2 to preserve pH 7.4 (Tang and Frojmovic, 1977). The PRP (1:10) was diluted 10-fold with Walsh-albumin buffer (140 mM NaCl, 2.7 mM KCl, 0.4 mM Na_2CO_3, 2 mM $MgCl_2$, 0.1% Glucose, 0.1% BSA, pH 7.4), to yield PRP (1:10) used for protein binding and aggregation studies.

Washed platelet suspensions

Washed platelet suspensions (WP) were prepared by a single-step centrifuging procedure (Goldsmith et al., 1994). PRP was acidified to pH 6.5 with 1.4% citric acid in 50 ml plastic tubes. The stable prostacyclin derivative, ZK was added to PRP at 50 nM immediately before centrifuging at 800 × g for 15 min. The platelet pellets were resuspended in modified Tyrodes (136 mM NaCl, 2.7 mM KCl, 11.9 mM $NaHCO_3$, 0.36 mM NaH_2PO_4, 1.0 mM $MgCl_2$, 5.6 mM glucose, 0.35% BSA) to a final platelet count of 3–6 × 10^5 μl^{-1}.

Activated and fixed platelets

Preparation of AFP is similar to the method of Du et al. (1991). Washed platelets suspended in modified Tyrodes containing 10 nM ZK (1 × 10^6 cells·μl^{-1}) were incubated at 37°C for 35 min and for another 5 min with 1 mM $CaCl_2$. GRGDSP, which activates GPIIb-IIIa directly, was then added at a final concentration of 1 mM. The suspension was incubated for 5 min at 37°C. The activated platelets were fixed by adding the suspension to freshly prepared 1% paraformaldehyde (1:1 in volume). The suspension of activated, fixed platelets was then incubated at room temperature for 1 h, followed by washing (2X) at 150 × g and resuspending in Tyrodes-HEPES-albumin buffer (Tyrodes, 5 mM HEPES, 1% BSA, pH 7.4). The AFP suspension can be stored in Ca^{2+}-free Tyrodes-HEPES-albumin buffer (THA) at 4°C for at least a week without causing aggregation. Calcium (1 mM) was added to the working AFP suspensions just before experiments.

Protein binding

Micro-couette

A micro-couette composed of two concentric plexi-glass cylinders (Fig. 1) was used for protein binding and aggregation studies. The surfaces of micro-couette were siliconized with Surfasil (10-fold dilution in hexane) to minimize cell adsorption. The inner cylinder rotates at an angular velocity (w) with the outer cylinder stationary, to yield mean shear rates of 1–1000 s^{-1}, determined from $G = R \cdot w/h$, where R = 10.5 mm and the gap distance h = 0.5 mm, i.e., $G = 1.09w$. Suspensions (400 μl) were subjected to shear in the gap between the cylinders after brief (<2 s) premixing of all added reagents with a disposable Pasteur pipette before immersion of the inner cylinder. The entire suspension of 400 μl was taken for the flow cytometry analysis of bound proteins. For aggregation studies, shear was stopped at consecutive times for subsampling (40 μl) by micro-pipettes from the outlet on the side, after discarding a dead volume (20 μl). The subsamples were fixed immediately with a sixfold dilution in glutaraldehyde (0.67% v/v) for analysis in a particle counter (Elzone 80xy, Particle Data Inc., Elmhust, IL) (Frojmovic et al., 1989).

BSA on latex beads

The latex beads suspended in PBS (pH 7.4) at 23,000 ± 3,000 μl^{-1} were incubated in a micro-couette for varying times in the presence or absence of shear with FITC-labeled BSA. At the end of the incubation, the suspension was transferred into polystyrene tubes, and the mean fluorescent intensity, FL, was then measured by a flow cytometer, FACScan (Becton Dickinson, Mississauga, Ontario) within a few seconds. To minimize adsorption of the labeled BSA onto the surfaces of the micro-couette, the

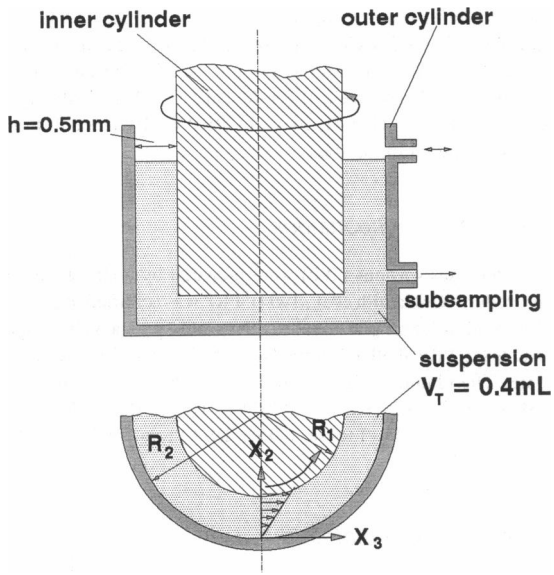

FIGURE 1 Micro-couette. A micro-couette composed of two concentric plexi-glass cylinders of respective diameters of 10 mm (o.d.) and 11 mm (i.d.), with a gap $h = 0.5$ mm. The inner cylinder, driven by a high precision step motor, rotates at a desired angular velocity, with respect to the stationary outer cylinder, to yield a simple shear flow in the space between the confining cylinders with a mean shear rate ranging from 1 to 1000 s^{-1}. Suspensions of 400 μl are added from the top of the couette after lifting the inner cylinder, whereas the subsamples (40 μl) are collected from the outlet on the side, after inserting the inner cylinder, and discarding a dead volume (20 μl) before each subsampling. Because the outlet is above the bottom surface of the inner cylinder, the volume at the bottom of the couette is not sampled.

couette was precoated with 1% unlabeled BSA (in PBS) for 2 min, followed by rinsing with PBS (3X) before introducing a suspension. Shearing the PBS buffer at 300 s^{-1} for 5 min only caused negligible amount of BSA to reappear in the buffer, as measured by o.d., representing <5% of labeled BSA used for binding studies.

PAC1 on platelets

PAC1 (Shattil et al., 1985) was used to determine the effect of shear on the kinetics of its specific binding to activated GPIIb-IIIa. PRP was diluted with platelet-poor plasma and Walsh-albumin buffer so that the platelet concentration was 6000 μl^{-1}, and final protein concentration was 1/10 of that in PRP. Platelets were activated with 100 μm ADP for 2 min in the BSA precoated micro-couette (390 μl), followed by addition of 10 μl of FITC-labeled PAC1 (15 nM final). The time course of the binding of FITC-labeled PAC1 was carried out by measuring *FL* of the suspensions at the end of incubation periods varying from 0.5 to 30 min, in the presence or absence of shear of 300 s^{-1}. *FL* for nonspecific binding was estimated by the addition of 1 mM (final concentration) GRGDSP before ADP. FL due to specific binding was defined as FL in absence of GRGDSP less that in presence of GRGDSP.

Fibrinogen on AFP

Kinetic binding of FITC-labeled human fibrinogen (FITC-Fg) on activated and fixed platelets in modified Tyrodes was performed in the absence of flow without further activation of the platelets. The fibrinogen is von Willebrand factor (vWF)-free, and was labeled with fluorescein isothiocyanate, as described elsewhere (molar F/P = 3.9); the working molar F/P was 1.3 by threefold dilution with unlabeled Fg to minimize surface self-quenching (Z. Xia, T. Wong, and M. M. Frojmovic, unpublished data). For equilibrium binding at pH 7.4, diluted suspension of AFP (5000/μl) was incubated, in the dark, with FITC-Fg at various concentrations (10–1 mM) for 1 h at room temperature. Fluorescence intensity for nonspecific binding was determined by adding 1 mM GRGDSP to the suspension before the addition of FITC-Fg. Specific FL was total FL minus nonspecific FL. The percent of Fg occupancy at time t was determined by comparing *FL* of specifically bound FITC-labeled Fg at that time with the maximum specific FL obtained from the equilibrium binding.

Estimation of percent of GPIIb-IIIa activation

PRP (1:10) was incubated with FITC-Fg (350 μM) with ADP of various concentrations for 40 min at room temperature. The ratio of specific *FL* to FL_{max} obtained at 100 μm ADP, was defined as the apparent percent of GPIIb-IIIa activation of the suspension. Previous work in this lab (Frojmovic et al., 1993) showed that subpopulations of platelets exist that are either maximally activated or unactivated, and that the activated subpopulation increases with ADP concentration. Thus, this ratio is also equivalent to the fraction of fully activated platelets.

Determination of the kinetics of platelet aggregation

Platelets activated either by ADP or GRGDSP were subjected to shear in a micro-couette under a desired shear rate (100–1000 s^{-1}). At time t, the suspensions were subsampled and analyzed by measuring the change in platelet particle number per unit volume with the Elzone resistive particle counter (Model 80XY, Particle Data Inc.), as previously described (Frojmovic et al., 1989). The fraction of particles recruited into aggregates, *PA*, was calculated using the equation

$$PA = \left(1 - \frac{N_t}{N_o}\right), \tag{1}$$

where N_t and N_o are platelet number concentrations determined by counting particles in the subsamples taken at $t = t$ and $t = 0$, respectively.

Determination of capture efficiency

Capture efficiency is defined as the fraction of shear-induced collisions between two platelets that result in doublets, i.e., the ratio of the rate of the measured initial aggregate formation for dilute suspensions (dN_t/dt) to the frequency of two-body collisions in the suspension. The Smoluchowski (Smoluchowski, 1917) collision frequency of a suspension, *CF*, is given by

$$CF = \frac{16}{3} G N_t^2 a^3, \tag{2}$$

where G is the shear rate and a is the equivalent spherical radius of platelets. Therefore, the capture efficiency can be expressed as

$$\alpha = \frac{dN_t/dt}{(16/3)Ga^3N_t^2}. \tag{3}$$

Combining Eq. 1 and the integrated form of Eq. 3 gives the initial rate of aggregation as

$$\left.\frac{dPA}{dt}\right|_{t\to 0} = \frac{16}{3}\alpha G a^3 N_o. \tag{4}$$

The initial rate of aggregation can be obtained experimentally by finding the best fit of *PA* values at time t to the equation

$$PA = PA_{max}(1 - e^{-t/B}), \tag{5}$$

where the initial rate of aggregation is PA_{max}/B. Hence, α values can be calculated from Eq. 4.

We confirmed by direct particle counting by microscopy (Frojmovic et al., 1989) that *PA* values were (i) identical to *PA* measured by particle counting, and (ii) that early microaggregation for $PA \simeq 30\%$ consisted only of doublets (20%) and triplets (10%) ($n = 2$). In the absence of ADP activation, "insignificant" aggregation with shear typically corresponded to $PA = 9 \pm 4\%$ (mean ± SD) ($n = 6$ determinations on the same sample for $N_0 = 40{,}000/\mu l$).

RESULTS

Effect of shear on dynamic binding of proteins to latex beads

FITC-labeled albumin was used as a model protein to evaluate the shear dependence of adsorption/desorption to carboxylated latex spheres of similar size as human platelets (2.01 μm diameter). The mean *FL* of gated singlets of these latex suspensions increased rapidly with a half-maximum time ($t_{1/2}$) of <20 s, then increased gradually, with a tendency of plateauing, regardless of shear (Fig. 2 *a*). The decreases in *FL* between samples at rest and those sheared at $t \leq 30$ s is within the experimental error. However, the suspensions under shear showed significantly lower *FL* at $t > 30$ s. Thus, the differences in *FL* due to shear at 700 s^{-1} and at 300 s^{-1} within 10 min were less than 33 and 18%, respectively, compared to samples at rest.

These shear-associated lower equilibrium values for bound albumin might arise from protein desorption. Therefore, we assessed the desorption rate. Latex beads preadsorbed with 1.23 μM FITC-BSA in a polypropylene tube at room temperature for 10 min were diluted 10-fold by PBS and transferred to the BSA-precoated micro-couette, where they were under shear at 300 s^{-1}. *FL* of gated singlets in the suspensions at varying durations of shear are shown in the inset of Fig. 2 *a*. *FL* of the suspensions only dropped by 5% due to desorption of FITC-BSA after 10 min of shear. Therefore, the 18% difference in *FL* during adsorption due to shear cannot be attributed to the shear-induced desorption.

Shear has been shown to enhance the rate of cross-bridging of latex beads partially coated with polymers, with highest cross-bridging efficiency at 50% of surface coverage (van de Ven, 1989). Thus, *FL* of the singlets in a suspension could be underestimated if the subpopulation of beads that have preferentially adsorbed BSA proteins formed aggregates. To investigate the possible bias in the analysis, *FL* of gated aggregates of the suspensions incubated with 425 nM FITC-labeled BSA are shown in Fig. 2 *b*. Percent of aggregates increased from 7 to 17% in 10 min for both the nonsheared or the sheared suspensions, i.e., insignificant difference. The mean intensities of forward scattering and side scattering of the aggregates were nearly twice the values of the singlets, regardless of shear, indicating that most of the aggregates were doublets. Furthermore, through the course of 10-min adsorption, *FL* values for the samples subjected to shear were also lower than the unsheared sample, the same trend found for singlets. This implied that the latex beads aggregated due to shear did not have preferential adsorption of BSA. Therefore, *FL* in Fig. 2 *a* were not underestimated.

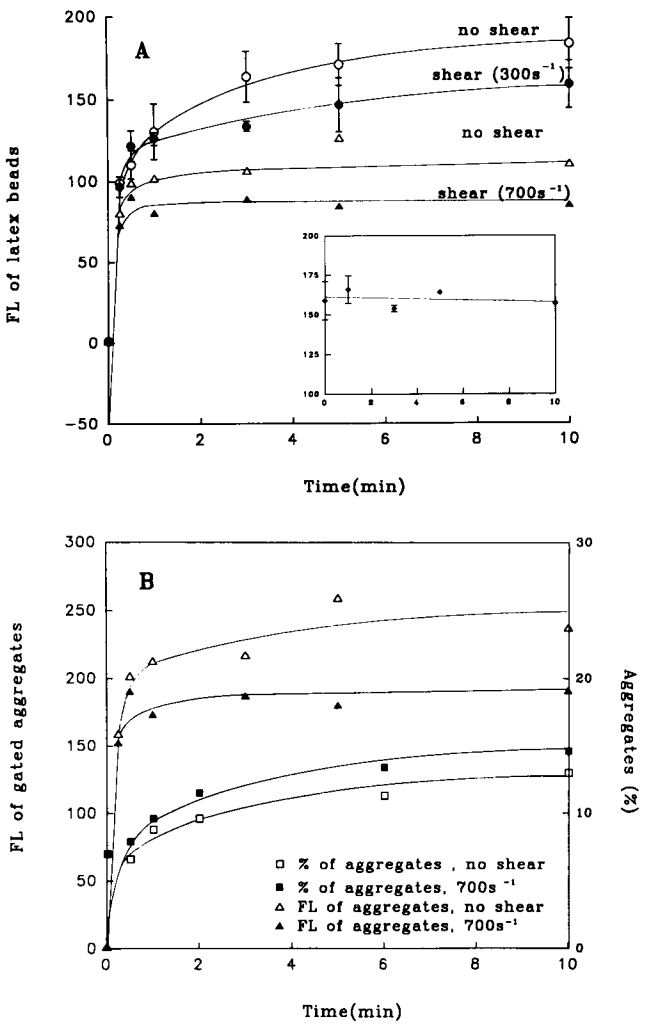

FIGURE 2 Effect of shear on dynamic binding of albumin to polystyrene beads. Latex suspensions were incubated with either 520 nM (○, ●) or 425 nM (△, ▲) FITC-labeled BSA at room temperature in the absence (○, △) or presence of shear at 300 s^{-1} (●) and 700 s^{-1} (▲). Latex particle concentrations varied from 20,000 to 28,000 μl^{-1}. The error bars represent SD of two independent experiments. (*A*) Fluorescent intensity of gated singlets in the latex suspensions at various incubation time. (*Inset*) Fluorescent intensity of beads pre-adsorbed with FITC-labeled BSA. The beads suspended in PBS at a concentration of 29,000 μl^{-1} were incubated with 1.23 μM FITC-BSA in a polypropylene tube at room temperature for 10 min. The suspension was diluted 10-fold by PBS and transferred to the BSA-precoated micro-couette, where it was under shear at 300 s^{-1}. (*B*) Fluorescent intensity of gated aggregates in the suspensions and percent of aggregates at the end of incubation with (■) or without (□) shear at 700 s^{-1}.

PAC1, IgM molecules that have larger molecular mass (900 kDa) and, thus, lower diffusion rates than BSA (79 kDa), and that bind specifically to ADP preactivated GPIIb-IIIa on platelets without causing cross-bridging, were also used for measuring shear-dependent kinetics of adsorption on platelets suspended in one-tenth of citrated plasma. *FL* values of FITC-labeled PAC1 on platelets at varying periods of adsorption are shown in Fig. 3. Adsorption, either nonspecific or total binding for the activated GPIIb-IIIa receptor,

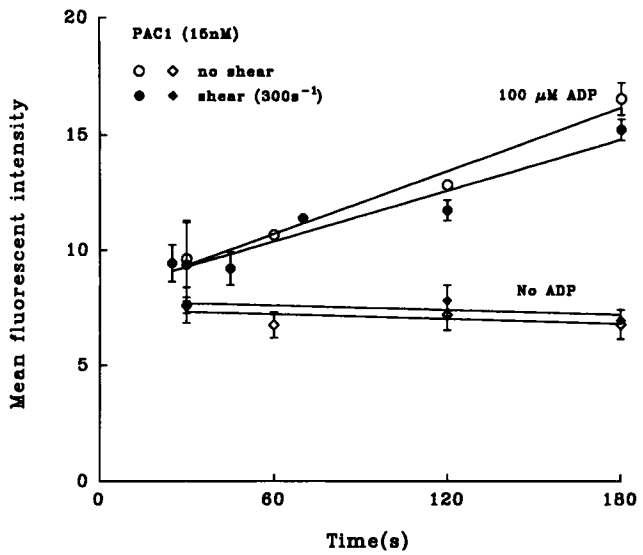

FIGURE 3 Effect of shear on dynamic binding of PAC1 to normal platelets. ADP-activated (○, ●) or nonactivated (◇, ◆) platelets (6000 μl^{-1} final) were incubated with 15 nM FITC-labeled PAC1 in the BSA pre-coated micro-couette in the presence (●, ◆) or absence (○, ◇) of shear (300 s^{-1}). Each symbol represents the average of two independent samples, with an SD indicated by an error bar. Lines are linear regression of the data points.

was found to be the same for no shear or shear at 300 s^{-1} over the first 3 min of adsorption.

Quality of activated-fixed platelets

Preparation of GRGDSP-activated and paraformaldehyde-fixed platelets (AFP) enable us to activate GPIIb-IIIa before exposure to a known quantity of Fg molecules and without secondary complications associated with physiologic activation and secretion. To assess the quality of each preparation, the activity of GPIIb-IIIa on AFP was tested by incubating AFP (20,000–30,000 μl^{-1}) with a variety of ligands, including FITC-PAC1 (40 nM, F:P 8.5), FITC-Fg (500 nM, F:P 3), Fg (500 nM)/FITC-9F9 (250 nM, F:P 9), and FITC-S12 (100 nM, F:P 10). At the end of incubation in the presence of 1 mM $CaCl_2$ and 1 mM $MgCl_2$ at room temperature for 40 min, the samples were analyzed for mean fluorescent intensity by flow cytometry. The control samples contained 1 mM GRGDSP in addition. The results for a representative preparation are shown in Fig. 4. The mean fluorescent intensity for FITC-PAC1 is 112 with a control (containing GRGDSP) at ~15 (Fig. 4 *a*). *FL* for FITC-9F9 in the presence of Fg and Fg/GRGDSP and in the absence of Fg is, respectively, 493, 17, and 20 (Fig. 4 *b*). *FL* for FITC-Fg in the presence and absence of GRGDSP is ~25 and 466, respectively (Fig. 4 *c*). Apparently, the binding of both PAC1 and Fg can be inhibited by GRGDSP. The data suggest that: >90–95% of all AFP express maximum number of activated GPIIb-IIIa receptors (Fig. 4 *a*); negligible secreted/bound Fg (Fig. 4 *b*); maximal binding by all platelets of extrinsically-added Fg (Fig. 4 *c*); and negligible secretion of α-granules with AFP preparation (Fig. 4 *d*). AFP suspensions contained ≤5% aggregates, mostly doublets, readily gated out in flow cytometric analyses. Pseudopods were observed on 80% of singlet platelets, although platelets remained discoid shaped. The secretion is considerably less than that from platelets obtained by gel filtration

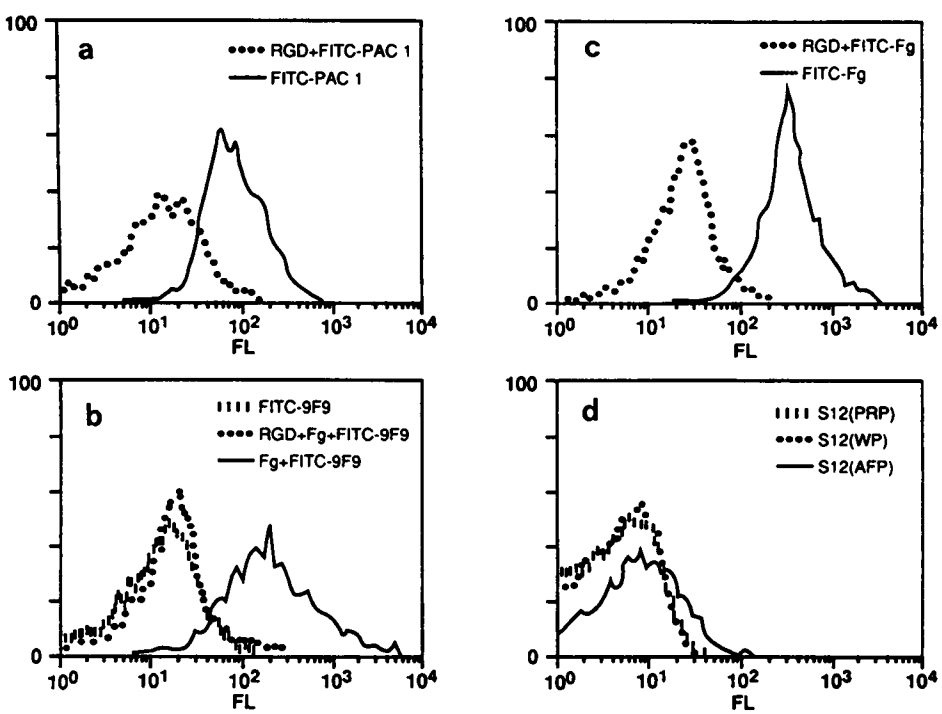

FIGURE 4 GPIIb-IIIa receptors on AFP maintain the fibrinogen binding function. AFP in modified Tyrodes (20,000–30,000/μl) were incubated with the following ligands without further activation for 40 min at room temperature before being analyzed with flow cytometry: (*a*) FITC-PAC1, monoclonal antibody (IgM) specific to activated GPIIb-IIIa; (*b*) FITC-9F9, monoclonal antibody against GPIIb-IIIa bound Fg, after the addition of Fg; and (*c*) FITC-Fg. The control in each case was addition of 1 mM GRGDSP, an RGD equivalent peptide that blocks activated GPIIb-IIIa. Final concentrations: FITC-Fg: 500 nM; Fg: 500 nM; FITC-PAC1: 40 nM; FITC-9F9: 250 nM, GRGDSP: 1 mM, $CaCl_2$: 1 mM, $MgCl_2$: 1 mM. Fluorescent intensity of FITC-S12 (100 nM final), antibody specific to platelet α-granule membrane protein GMP 140, for AFP, WP, and resting normal platelets is shown in *d*.

in our hands, which yield >50% of GMP-140 expression (compared to maximal expression found with 0.2 μM PMA).

AFP stored in modified Tyrodes, with or without 0.01% NaN_3, at 4°C for at least one week, showed less than 5% decrease in the fluorescent intensities of bound FITC-Fg, FITC-9F9/Fg, and FITC-PAC1, indicating that GPIIb-IIIa remained activated for at least a week. AFP prepared from PRP instead of from washed platelets also showed comparable mean fluorescent intensities for all reporting probes (data not shown).

AFP from both WP and PRP stirred in a aggregometer at 1000 rpm for 2 min yielded similar *PA* values (~50%), consistent with the values for 100 μm ADP-activated PRP, although the initial rate and maximal extent of aggregation of AFP measured by light transmittance in an aggregometer is only 40 and 20%, respectively, of those for ADP-activated PRP due to relatively smaller aggregates (seen with a microscope).

Binding of fibrinogen to activated-fixed platelets

The dissociation constant, K_D, of fibrinogen bound to AFP was estimated to be 77 nM from equilibrium binding experiments using the method of Scatchard; the maximum number of Fg binding sites were estimated as 64,000 per AFP (Z. Xia, T. Wong, and M. M. Frojmovic, unpublished data).

Kinetic adsorption of FITC-Fg on AFP was performed at room temperature in a series of polypropylene tubes containing 350 μl AFP (20,000–22,000 μl^{-1}, final) and 300 or 700 nM FITC-Fg. The suspensions were analyzed successively at desired time by flow cytometry. In the absence of shear, *FL* due to specific binding of FITC-Fg on AFP increased approximately exponentially with time for both FITC-Fg concentrations (Fig. 5). The maximum *FL* for both FITC-Fg concentrations obtained from the best fit for the experimental curves (183 and 300) were in good agreement with the values obtained from the equilibrium binding experiments (167 and 346), within experiment error. The time to reach half of the maximum *FL*, $t_{1/2}$, is 2.6 and 2.7 min for Fg concentrations of 300 and 700 nM, respectively.

Capture efficiency of normal platelets and activated-fixed platelets

Citrated PRP was diluted with Walsh-albumin buffer (pH 7.4) and platelet poor plasma (PPP) to yield varying platelet number concentrations with the same plasma concentration. The fraction of platelets recruited into aggregates, *PA*, at time *t* for three platelet concentrations, at shear rate 250 s^{-1}, are shown in Fig. 6. The time course of aggregation can be well described by Eq. 5, indicated by lines in the figure. The initial rates obtained by finding the best fit of the first four experimental values instead of all seven values did not change significantly (<15%), whereas the experimental error can be as high as 30%. Therefore, the initial rate and, thus, the efficiency of aggregation can be evaluated by subjecting the suspensions to shear for only 30 s.

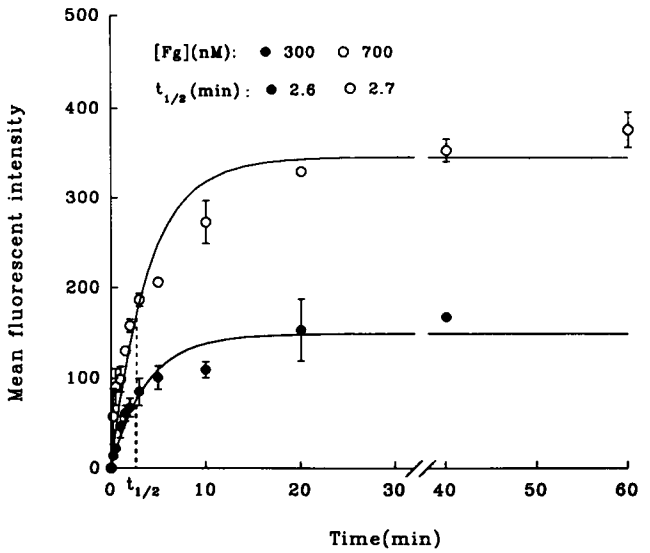

FIGURE 5 Kinetics of fibrinogen binding on AFP. Fluorescence intensity (mean of two samples) of AFP suspensions exposed to 300 nM (○) or 700 nM (●) FITC-Fg for various time were fit to exponential equations (*lines*). Nonspecific adsorption, measured from the samples containing Fg and 1 mM GRGDSP, were subtracted. $t_{1/2}$ is 2.6 and 2.7 min for [FITC-Fg] of 300 and 700 nM, respectively.

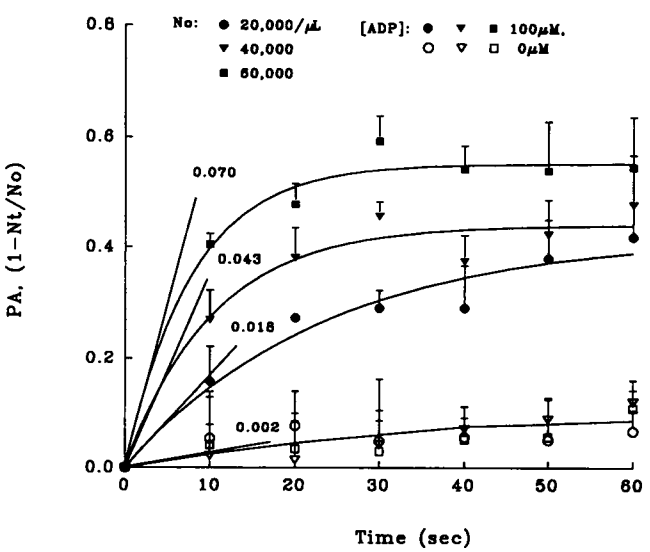

FIGURE 6 Linear dependence of initial aggregation rate on platelet concentration. Suspensions with the same plasma concentration and three different number concentrations of regular platelets were subjected to shear of 250 s^{-1}. The fraction of the platelets recruited into aggregates, PA, varied with time *t*. Symbols represent mean values of duplicate experiments for resting platelets (*open symbols*) and maximally activated platelets (*closed symbols*) by incubating with 100 μM ADP for 2 min at room temperature. The curves are the best fit ($r = 0.85$) to the equation $PA = PA_{max}(1 - e^{-t/B})$, with the slopes indicating initial aggregation rates.

Nonspecific aggregation (in the absence of ADP) is negligible (<10%), as is the diffusion-driven ($G = 0$ s^{-1}) aggregation. The correlation between the initial aggregation

rate and the platelet concentration N_0 is approximately linear ($r = 0.87$) at the fixed shear rate evaluated ($G = 250\ s^{-1}$).

Increasing shear rate G by 10-fold from 100 to 1000 s^{-1}, caused a fivefold drop in capture efficiency α (from 0.32 to 0.06), for platelets in PRP (1:10) maximally activated with ADP. α approached zero as $G \rightarrow \infty$. Plotting α vs. $1/G$ (Fig.7) showed a linear range at $1/G < 0.005$ (or $G > 200$), seen by the best fit to the equation $\alpha = 53 \cdot G^{-1}$.

Because GPIIb-IIIa activation is generally considered a prerequisite for platelet aggregation, the degree of GPIIb-IIIa activation was also expected to affect aggregation efficiency. To evaluate this effect, PRP (1:10) (40,000 cells μl^{-1}) was activated with various concentrations of ADP before shearing at 400 s^{-1}. It has been observed (Frojmovic, 1993) that platelet subpopulations respond quantally to ADP, i.e., the fraction of fully activated platelets expressing maximal numbers of fibrinogen receptors increases directly with increasing ADP concentration, and can be determined directly from changes in mean fluorescence for the total population for PAC1 or Fg binding. FL/FL_{max} at various ADP concentrations was taken as the apparent percent of GPIIb-IIIa activation, FL_{max} being the mean fluorescent intensity of maximally activated platelets (by 100 μM ADP). The apparent efficiency was determined assuming that all the platelets can participate equally in aggregation whether resting or activated, shown in Fig. 8. α increased linearly from 0.02 to 0.12, as ADP varied from 0.5 to 100 μM, corresponding to a slope of unity.

To assess the aggregation efficiency as a function of varying occupancy of fully activated GPIIb-IIIa by Fg, a more uniform platelet population, "RGD" activated-fixed platelets were used and the percent of Fg occupancy, instead of ADP concentration, was varied (Fig. 9). The varying of levels of Fg occupancy was achieved either by changing Fg concentration at a fixed (2 min) incubation time (occupancy < 50% in Fig. 9) or by changing incubation time at a fixed Fg concentration (occupancy > 50% in Fig. 9). Fluorescence his-

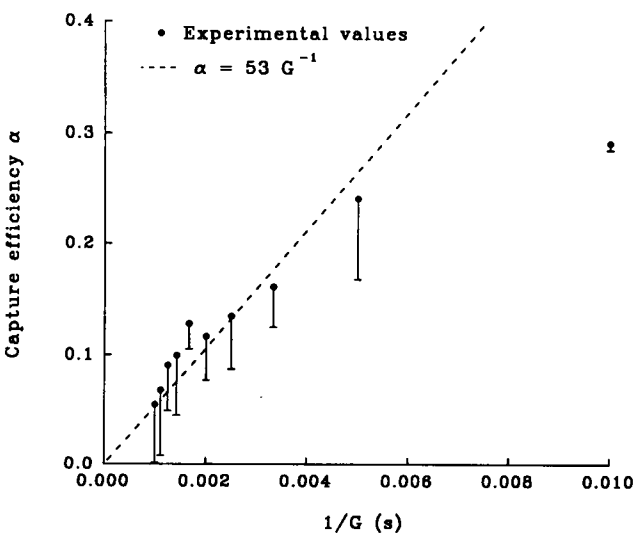

FIGURE 7 Capture efficiency of maximally preactivated PRP (1:10) at various shear rates. The capture efficiency α for platelets in PRP (1:10) maximally activated by incubating with 100 μM ADP for 2 min (*symbols*) varied with the inverse shear rate G^{-1}, as the shear rate G increased from 100 to 1000 s^{-1}. Line is the linear regression of the experimental values.

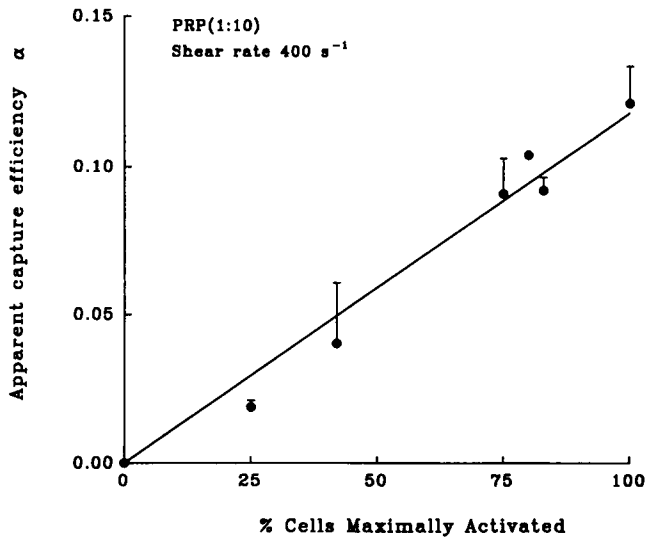

FIGURE 8 Capture efficiency of PRP (1:10) at various degrees of GPIIb-IIIa activation. The apparent efficiency of partially activated PRP (1:10) (40,000 μl^{-1}) at a shear rate of 400 s^{-1} increased with percent of activated GPIIb-IIIa achieved by varying concentrations of ADP from 500 nM to 100 μM in the preincubation. The percent of maximally activated platelets, due to subpopulation behavior, was calculated from the mean fluorescent intensity of the partially activated platelets incubated with 500 nM FITC-Fg for 40 min, taking FL for 100 μM ADP incubation as 100% GPIIb-IIIa activation. Symbols represent the mean of two experiments. The line is a linear regression with a constraint $\alpha = 0$ for 0% GPIIb-IIIa activation.

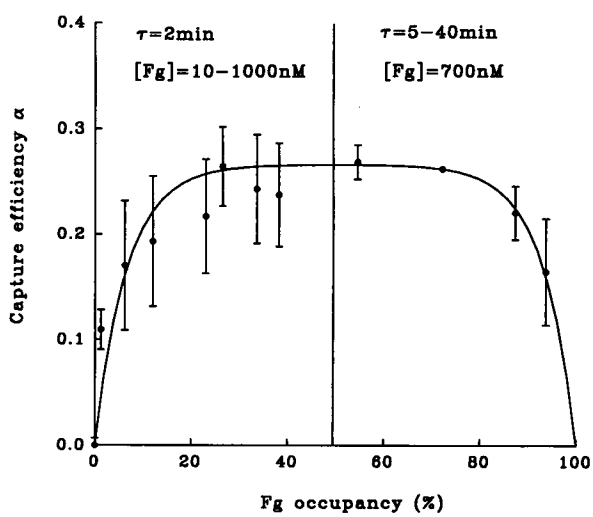

FIGURE 9 Capture efficiency of platelets with varying fibrinogen occupancy at a fixed shear rate (300 s^{-1}). Fg occupancy was defined as the ratio of the mean fluorescent intensity of the bound FITC-Fg of the suspensions to that of maximum FL from Fig. 5. Low Fg occupancy (<50%) was achieved by incubating AFP with Fg of various concentrations (10–1000 nM) for 2 min, whereas high occupancy (>50%) was obtained by varying incubation time (τ) at a fixed Fg concentration (700 nM). The line is the best of fit to an exponential equation to the experimental values (mean of two experiments, each having duplicates) for $\alpha > 50\%$ and its mirror image for $\alpha < 50\%$ (mean of six experiments, each having duplicates).

tograms for FITC-Fg binding showed no sub-population behavior, but rather partial binding to all platelets. The Fg occupancy was calculated from the fluorescent intensity of the suspensions, compared to 100% occupancy for incubation at 1 μM FITC-Fg for 40 min. Capture efficiency α, at $G = 300$ s^{-1}, increased with percent of Fg occupancy and reached a plateau value of approximately 0.25, with half-maximum of α occurring at only around 3% occupancy. α remained constant from 25 to 75% Fg occupancy, and decayed at higher Fg occupancy. The maximum efficiency of AFP is comparable with that of (1:10), maximally preincubated with ADP at the same shear rate (Fig. 7).

Molecular basis of aggregation

Because the data in Fig. 9 suggest that full occupancy of all Fg receptors will not allow platelet-platelet cross-bridging, we next sought to assess the importance of free fibrinogen receptors in Fg-mediated platelet aggregation. Fig. 10 shows inhibition of aggregation by GRGDSP and its nonpeptide analog Ro 43–5054. Identical extent of aggregation was found for platelet suspensions sheared at 300 s^{-1} for 30 s whether using PRP (1:10) activated with ADP (38,000 μl^{-1}) or Fg preincubated AFP (36, 500 μl^{-1}) ($PA = 0.57 \pm 0.01$). Adding 1 mM GRGDSP to PRP (1:10) immediately before ADP, or to AFP suspensions before 500 nM Fg, resulted in a fivefold decrease in *PA*. These low *PA* values were comparable to those of the resting PRP (1:10) and Fg-free AFP suspensions, but this procedure blocked specific Fg binding in both cases. However, adding GRGDSP at the end of ADP or Fg incubation equally minimized *PA*; however, there was no significant reversal in the Fg occupancy due to inhibitor addition: ~50% occupancy for either PRP (1:10) or AFP under the condition used (Fig. 10). Similar inhibition effects were achieved by replacing GRGDSP with 500 nM nonpeptide analog Ro 43–5054 for PRP (1:10), and with 100 nM Ro 43–5054 for AFP suspensions.

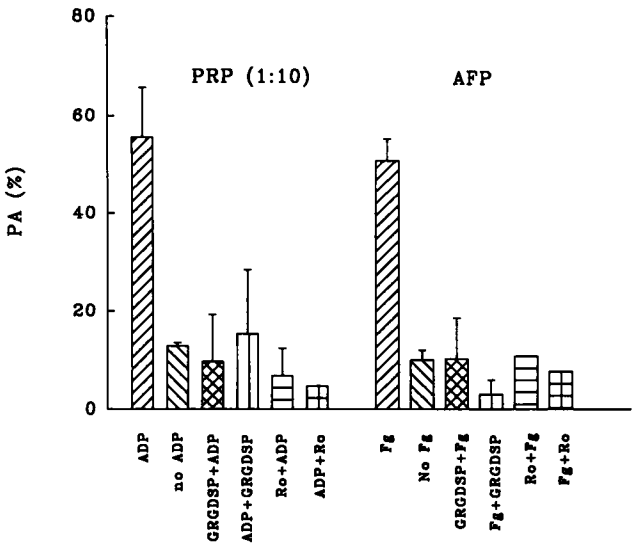

FIGURE 10 Inhibition of platelet aggregation by GRGDSP and its analog. PRP (1:10) with platelet concentrations of 38,000 μl^{-1} or AFP of 36,500 μl^{-1} were allowed to aggregate under shear (300 s^{-1}) in a micro-couette for 30 s. PRP (1:10) was maximally activated with 100 μM for 2 min before shear. AFP was also preincubated with 500 nM of Fg for 2 min. The inhibitors, GRGDSP (1 mM) or Ro 43–5054 (100 nM in AFP and 500 nM in PRP (1:10)), were added either before or after ADP or Fg incubation.

DISCUSSION

Proteins and latex beads in simple shear flow undergo both Brownian motion and shear-driven convection. For proteins, the ratio of the effect of shear to that of diffusion, denoted by the Peclet number (*Pe*), is given by $Pe = a_p^2 G/D_p$, where a_p and D_p are the respective radius and translational diffusion coefficient of a protein molecule, and G is the shear rate. The values of *Pe* at $G = 700$ s^{-1} for proteins of the equivalent spherical radii between 10 and 100 nm, such as albumin, IgM, and Fg, are on the order of 0.01–0.1. Therefore, the shear-driven movement of the protein molecules should be expected to make only negligible (1%) contributions to the collision frequency between albumin and latex beads. On the other hand, the shear-driven movement of the latex beads may enhance the collision between the beads and protein. The rate of diffusion-driven collision, J_d, for a reference bead of radius a_b and diffusion coefficient D_b, with proteins of number concentration N_p is given by $J_d = 4\pi N_p(D_b + D_p)(a_b + a_p)$ (DeWitt and van de Ven, 1992), whereas shear driven collision, J_s, is given by $4/3(1 + q)^3 N_p G a_b^3$, where $q = a_p/a_b$. The ratio of J_s to J_d is approximated to $Peq/3\pi$, assuming $D_b \ll D_p$. At a shear rate of 300 s^{-1}, *Pe* of a latex bead of 2.01 μm in radius is 1400 and q is estimated to be around 0.005, assuming albumin molecules have an equivalent spherical radius of 0.5 nm. Thus, the J_s/J_d is of the order of 0.75. The ratio of experimental adsorption rates in the presence of shear to that in the absence of shear is expected to be $1 + J_s/J_d$, i.e., 1.75, provided that shear driven binding efficiency is the same as the diffusion driven one.

Calculations (Cox et al., 1968) of hydrodynamic trajectories of two unequal-sized spheres in simple shear, in the absence of Brownian motion, external forces, and multibody interaction, predict that the spheres are unable to approach each closer than a distance d_{min}, which is given as $0.16a_b$ if $q \to 0$. Consequently, shear alone cannot bring proteins of 100 nm in radius into contact with latex spheres (1 μm in radius), although it increases the flux of protein at d_{min} and thus reduces the diffusion distance. Therefore, shear is effective only when the average distance between a protein and a bead is smaller than d_{min}. The values of d_{min} may change in the presence of colloidal forces, however not substantially, because the van der Waals attraction between a protein and a latex particle is weak and the electrostatic repulsion in physiological buffer is also negligible. d_{min} may also alter for rough surfaces.

The rate of adsorption of albumin has been shown (Lee and Kim, 1974) to change little with flow rate for one hydrophobic substrate (e.g., silastic rubber), although maximal binding increased almost sevenfold, whereas the rate of adsorption decreased more than 10-fold with increasing flow

rate for another substrate (e.g., copolyether-urethane-urea) with the same maximal binding. These differences were attributed to shear effects on relative contributions of hydrogen bonding, colloidal interactions, and surface roughness. However, we have shown that shear at both 300 and 700 s^{-1} did not increase adsorption rates of albumin to latex beads, contrary to the above predicted nearly twofold increase. The mean bead/protein distance is much greater than d_{min} under our experimental conditions, because the average protein-protein and bead-bead distances in the solution are estimated to be 150 nm and 33 μm, respectively. Therefore, an effect of shear is expected. However, if flux of protein at distance d_{min} from a latex bead increases with shear rate, the adsorption rate should be proportional to G, which we have not observed. It is also unlikely that collision frequency is increased at the cost of reducing the efficiency of adsorption, due to shorter contact time, because efficiency would have to be exactly compensated by the enhancement of adsorption rate by shear-induced collisions at one particular shear rate (e.g., 300 s^{-1}) but not at another (e.g., 700 s^{-1}). Moreover, PAC1 molecules that have both different affinity and q also fail to show any differences due to shear. Platelets having oblate spheroidal shape and rough glycocalyx on the surface showed no proof of reducing d_{min}. Therefore, the effect of shear on protein adsorption via the convective movement of the beads appears to be negligible.

Studies on von Willebrand factor (vWF) adsorption revealed that these extremely long and thin filaments adsorb faster at higher shear rate onto latex particles over the period of 4 min (Furlan et al., 1987). However, this increase in adsorption rate due to shear is less than twofold, despite of a fivefold increase in shear (500 to 2500 s^{-1}). It may not be attributed to the increase in collision frequency but probably results from altered capture efficiencies due to changes in conformation of vWF (Roth, 1992) and resultant exposure of more binding sites. In addition, von Willebrand factor molecules are highly polydispersed. Albumin, on the other hand, is a more rigid spheroidal protein and monodispersed, thus behaving differently from vWF under shear.

The lower extent of adsorption of albumin onto latex beads in the presence of shear could be due to a higher detachment rate in presence of shear. Although the detachment rate measured at the end of 10-min adsorption is negligible, early desorption may occur with shear. This would be consistent with a report (Brash and Samak, 1978) that albumin molecules adsorbed on polyethylene tubing measured in $\leq$4 min exchanges with those in solution with a higher rate at increasing shear rates.

The direct measurements of dynamic binding of Fg on AFP as a function of shear has proven experimentally unfeasible to date, due to the difficulty in interpreting FL of the mixture of singlets and shear-induced aggregates. However, it is anticipated that the dynamic binding of fibrinogen, which has molecular weight between those of BSA and PAC1, and which binds to GPIIb-IIIa analogous to PAC1, will not be affected by shear under our experimental hydrodynamic conditions. However, direct effects of shear on Fg conformation and affinity to its platelet receptor must still be evaluated.

Because shear will have little influence on dynamic protein binding in the absence of any direct effects on protein conformation and adhesiveness, the kinetic studies of platelet aggregation can be pursued by pre-incubation of agonists in the presence of adhesion molecules like Fg without shear, followed by contributions of shear to platelet-platelet interactions.

Both kinetics and equilibrium fibrinogen binding have been traditionally carried out with ^{125}I-labeled fibrinogen on gel-filtrated platelets (Bennett and Gaston, 1979; Plow and Marguerie, 1980). Using ^{125}I as probes could introduce complications due to the pelleting of platelets to remove the unbound Fg. Gel filtration of platelets, in our experience, causes major granule secretion and release of intracellular fibrinogen that may not participate in aggregation. In addition, platelet activation associated with "washing" (Goldsmith et al., 1994), or with ADP-induced activation of whole blood (Warkentin et al., 1990) or PRP (Frojmovic et al., 1993), yields a mixture of "resting" and "fully-activated" platelets, which, respectively, bind no significant and maximal numbers of activated GPIIb-IIIa captured Fg. Studies of Fg binding on "RGD"-activated, fixed platelets (AFP) using fluorescent probes, on the other hand, shows a uniform platelet population with maximally activated GPIIb-IIIa receptors, all uniformly binding Fg, and negligible granule secretion. These fixed platelets aggregate in the presence of Fg with no further activation, but fail to form the large aggregates seen with maximally activated unfixed platelets, which may require other participants in plasma or by secreted materials.

The time required to reach half-maximum binding of Fg on AFP is 2–3 min, similar to that reported for gel filtered platelets activated by either ADP or thrombin (4 min) (Plow and Marguerie, 1980). $t_{1/2}$ was almost constant despite a twofold increase in Fg concentration because of the large excess amount of fibrinogen in the solution. Because half-maximal binding occurred at 2–3 min, yielding about 50% occupancy, a 2-min incubation was used to achieve maximal rates of aggregation for this study of aggregation efficiency.

It was demonstrated that the initial rate of aggregation is proportional to the initial concentration of platelets, and follows second order kinetics. Because the efficiency α for the platelets in the same buffer conditions was a constant, the linear increase of the aggregation rate with N_o determined in our micro-couette obeys the Smoluchowski model given by $PA = 16/3N_oGa^3$. In other words, aggregation rate can simply be described by a product of collision frequency and capture efficiency, even though platelets are not solid spheres. The interpretation of capture efficiency is complex and model-dependent. It includes the corrections for the following factors: (a) hydrodynamic interactions between colliding platelets, which determine contact sector of trajectories and gap distance during the contact period, which is a function of

shear rate and platelet shape and surface projections (pseudopod length and density); (b) colloidal interactions, including van der Waals attraction and steric repulsion of glycocalyx on platelet membrane (electrostatic repulsion is negligible in physiological saline); (c) probability of fibrinogen bridging, which, in turn, is a function of the fibrinogen occupancy, activated GPIIb-IIIa density, and lateral mobility of the receptors (GPIIb-IIIa) and ligands (bound Fg); and (d) kinetics and affinity of the cross-bridging (Bell, 1978).

The fraction of the trajectory within which the gap distance is equal to or less then the length of a cross-bridge will change with varying shear rate with subsequent change in the capture efficiency. Our data showed clearly that α decays as shear rate increases over a range between 100 and 1000 s^{-1}. The same trend was found (Bell and Goldsmith, 1984) when infusing ADP into citrated PRP in Poiseuille flow at lower shear rates (<100 s^{-1}). Numerical trajectory analysis of colloidal spheres (van de Ven and Mason, 1977) with no specific interactions predicted that efficiency can be described as

$$\alpha = c_1 C_A^k, \qquad C_A = \frac{A}{36\pi\eta G a^3}, \tag{6}$$

where C_A is the orbital constant, A is the Hamaker coefficient, η is the medium viscosity, $k \simeq 0.18$, and $c_1 \simeq 1$. An independent study (Zeichner and Schowalter, 1977) resulted in a slightly different values for k (0.25) and c_1 (2). Therefore, $\alpha \propto G^{-k}$. In fact, $\alpha = 0.4G^{-0.25}$ assuming that $A = 5 \times 10^{-21} J$. The predicted value of α is expected to be lower if steric repulsion is considered. Our results can be fitted to $\alpha = 59\,G^{-1}$, indicating that the capture efficiency due to cross-bridging is much higher at the same shear rate, yet more susceptible to changes in G than what was predicted by Eq. 6.

To calculate the capture efficiency of biological cells via ligand/receptor chemical reaction, Potanin et al. (1993) incorporated a specific force due to cross-bridging, F_{bt}, into the force balance in their analytical expressions of efficiency based on lubrication theory. F_{bt} is a function of surface density, radii, lateral diffusion constant, and elasticity of both receptors and ligands. For reasonably assumed values of these parameters, the calculated efficiency falls approximately from 0.23 to 0.16 due to nonspecific interactions as G increases from 10 to 100 s^{-1}. They predicted a plateau region at intermediate shear rates (10–2000 s^{-1}) where α varies by only 15% as shear rate increased by two orders of magnitude. The predicted α due to nonspecific and specific interaction decays from 0.36 to 0.31, in agreement with their measured efficiency of PRP by light transmittance. We found, however, that the measured efficiency decayed markedly from 0.32 to 0.06. It is possible that the effect of shear on capture efficiency is underestimated by assuming spherical shape. The trajectory of two colliding oblate spheroids, such as platelets with average axis ratio of about 0.4 (Frojmovic and Milton, 1983) is different from that of two spheres. The rate of rotation of a spheroid in simple shear field oscillates with time, which tends to increase the average gap between two cells (Kim, 1986). As shear enhances the rotation of platelets, and thereby increases the gap between platelets up to some limits, it is anticipated that capture efficiency decays with shear faster than for spherical particles.

According to Potanin's model, capture efficiency is also a function of surface densities of both bound fibrinogen (ligands) and activated but unoccupied GPIIb-IIIa (receptors), assuming that fibrinogen cross-bridging GPIIb-IIIa complex on the adjacent platelets is the mechanism of aggregation. It was initially anticipated that at various ADP concentrations added to unfixed platelets at a fixed Fg concentration, the total number of activated GPIIb-IIIa (both Fg occupied and unoccupied) changes, so that the ratio of occupied to unoccupied receptors would change. However, recent studies (Frojmovic et al., 1993) showed that platelets are not uniformly activated in a graded manner by increasing ADP concentrations, but rather, an "all-or-none, quantal" response occurs with either maximally activated (P^*) or not activated (P^o) platelets, with the fraction P^*/P^o increasing with increasing ADP concentrations (0.2–10 μM). We have demonstrated that the apparent capture efficiency at 400 s^{-1} increases linearly with the percent of maximally activated platelets (P^*) (Fig. 8). Therefore, if only P^* can aggregate (i.e., $\alpha = 0$ for P^o), then the real collision frequency between two P^* values must be calculated based on the percent P^* actually present in the platelet suspension. The collision frequency between two P^* values is a product of the collision frequency for the whole suspension and the percent of P^*. This corrected efficiency was found to be 0.11 ± 0.02, constant for the entire range of ADP concentrations studied. This provides strong evidence that our assumption is valid that only P^* is participating in aggregation. Because ADP activation of platelets and receptor expression takes place maximally in a few seconds, and Fg concentration in PRP (1:10) is fixed and in 100 time excess of total GPIIb-IIIa on platelets, nearly 40% of GPIIb-IIIa on activated platelets are occupied at the end of 2-min incubation, regardless of the percentage of activated platelets. The occupied to unoccupied ratio on activated platelets is a constant, resulting in a constant capture efficiency. This efficiency is comparable to 0.13 in Fig. 7 at 400 s^{-1}.

The ratio of occupied to unoccupied GPIIb-IIIa will change with variation of Fg concentration for AFP. The predicted attractive force due to ligand/receptor cross-bridging between adjacent platelets, which balances hydrodynamic and colloidal forces, is proportional to the product of the surface concentration of bound ligand (GPIIb-IIIa-Fg) and receptor (GPIIb-IIIa) (Potanin et al., 1993). Therefore, if the total activated GPIIb-IIIa is constant, the efficiency is symmetric with respect to 50% Fg occupancy, with a maximum plateau value over a range of Fg occupancy around 50%. This is consistent with our experimental results (Fig. 9). α remains maximal (~0.24) over the range of 25–75% Fg occupancy, but decreases rapidly at higher or lower occupancies. Studies on aggregation rate of gel-filtered platelet in an aggregometer at various Fg concentrations at 37°C (Landolfi et al., 1991)

also showed a bell-shaped curve, with a maximum aggregation rate at around 1 μM added Fg, near 50% occupancy measured by ^{125}I-labeled Fg. However, these aggregation experiments were performed immediately after the addition of Fg, whereas bound fibrinogen was measured after 20-min incubation. This may explain the discrepancy in Fg concentration between our experiments and theirs. In our studies with AFP, 50% of increase in α occurs at $\leq$2% Fg receptor occupancy, indicating that a small number of bound fibrinogen molecules were sufficient to cause significant aggregation, as is required by the circulation system for the platelets to have a quick response to endothelium trauma.

Ro 43–5054 has a higher potency (2–10 times) than GRGDSP, and is thus an excellent inhibitor for Fg binding (Fig. 10). It is also three orders of magnitude more specific for GPIIb-IIIa than it is for $\alpha_{V_n}\beta_3$ (Kouns et al., 1992), the vitronectin receptor, whereas GRGDSP has higher specificity for $\alpha_{V_n}\beta_3$ than for $\alpha_{IIb}\beta_3$. The block of Fg binding and platelet aggregation by Ro 43–5054, as well as GRGDSP, confirms the predominant role for activated but unoccupied $\alpha_{IIb}\beta_3$ as the cross-bridging molecule for FgR-Fg molecules on adjacent platelets. Neither Ro 43–5054 nor GRGDSP displace Fg pre-bound to platelets maximally activated with ADP in PRP, or with AFP, but rather, they directly block GPIIb-IIIa unoccupied by Fg and thus block aggregation determined at shear rate of 300 s^{-1} (Fig. 10). This is a direct proof that a GPII-IIIa Fg links to an activated GPIIb-IIIa receptor, in addition to the decrease in α at occupancy $\geq$75% (Fig. 9). Furthermore, our data for α vs. ADP in PRP and $\%P^*$ suggests that P^* Fg has a low, if >0, value for α for capture by P^o (unactivated platelets). Thus, although activated and unactivated Chinese hamster ovary cells transfected with platelet GPIIb-IIIa receptors have been reported to aggregate in the presence of Fg under gyrotation ($\bar{G}$ was estimated at <10 s^{-1}) (Gawaz, et al., 1991), we predict that negligible aggregation will occur at $\bar{G} \geq 100\ s^{-1}$.

It is widely accepted that platelet aggregation is likely mediated via cross-bridging of GPIIb-IIIa on adjacent platelets by fibrinogen molecules. Both α and γ chains of fibrinogen molecules bear GPIIb-IIIa recognition domains (D'Souza et al., 1988, 1991; Hawiger et al., 1989; Plow et al., 1984; Timmons et al., 1989), with the two α and one γ domains implicated in aggregation of platelets (Hawiger et al., 1989), although other studies suggested a role in platelet aggregation for only γ chain carboxyl termini (Farrell et al., 1992), rather than α domains (Ugarova et al., 1993), and also a role for direct interactions between Fg molecules bound to their GPIIb-IIIa receptors (Plow and Marguerie, 1982; Zamarron et al., 1991). Because all of the above studies of aggregation have been conducted for stirred platelet suspensions, evaluation of the molecular interactions must be made in well defined shear fields.

The generous participation of Professor Theo van de Ven and the Pulp and Paper Research Institute in the design and manufacture of the micro-couette device is gratefully acknowledged. The authors also thank Truman Wong for the preparation of washed platelets, the measurement of fibrinogen binding on normal platelets, and other technical assistance; we also thank Dr. T. Weller and F. Hoffmann-La Roche Ltd. (Basel, Switzerland) for Ro 43–5054.

This research was supported by the Medical Research Council of Canada.

REFERENCES

Anderson, G. H., J. D. Hellums, J. L. Moake, and C. P. Alfrey. 1978. Platelet response to shear stress: changes in serotonin uptake, serotonin release, and ADP induced aggregation. *Thromb. Res.* 13:1039–1047.

Bell, D. N., and H. L. Goldsmith. 1984. Platelet aggregation in Poiseuille flow. II. Effect of shear rate. *Microvasc. Res.* 27:316–330.

Bell, G. I. 1978. Models for the specific adhesion of cells to cells. *Science.* 200:618–627.

Belval, T. K., J. D. Hellums, and R. T. Solis. 1984. The kinetics of platelet aggregation induced by fluid-shearing stress. *Microvasc. Res.* 28: 279–288.

Bennett, J. S., and V. Gaston. 1979. Exposure of platelet fibrinogen receptors by ADP and Epinephrine. *J. Clin. Invest.* 64:1393–1401.

Chang, H. M., and C. R. Robertson. 1976. Platelet aggregation by laminar shear and Brownian motion. *Ann. Biomed. Eng.* 4:151–183.

Cox, R. G., I. Y. Z. Zia, and S. G. Mason. 1968. Particle motions in sheared suspensions. XXV. Stream lines around cylinders and spheres. *J. Colloid Interface Sci.* 27:7–18.

D'Souza, S. E., M. H. Ginsberg, G. R. Matsueda, and E. F. Plow. 1991. A discrete sequence in a platelet integrin involved in ligand recognition. *Nature.* 350:66–68.

D'Souza, S. E., M. H. Gingsberg, T. A. Burke, S. C.-T. Lam, and E. F. Plow. 1988. Localization of an Arg-Gly-Asp recognition site within an integrin adhesion receptor. *Science.* 242:91–93.

DeWitt, J., and T. G. M. van de Ven. 1992. The effect of neutral polymers and electrolyte on the stability of aqueous polystyrene latex. *Adv. Colloid Interface Sci.* 42:41–64.

Du, X., E. F. Plow, A. L. Frelinger, III, T. E. O'Toole, J. C. Loftus, and M. H. Ginsberg. 1991. Ligands "Activate" Integrin $\alpha_{II}\beta_{III}$ (Platelet GPIIb-IIIa). *Cell.* 65:409–416.

Farrell, D. H., P. Thiagarajan, D. W. Chung, and E. W. Davie, 1992. Role of fibrinogen α and γ chain sites in platelet aggregation. *Proc. Natl. Acad. Sci. USA.* 89:10729–10732.

Frojmovic, M. M., J. G. Milton, and A. L. Gear. 1989. Platelet aggregation measured in vitro by microscopic and electronic particle counting. *Methods Enzymol.* 169:134–149.

Frojmovic, M. M., and J. G. Milton. 1983. Physical, chemical and functional changes following platelet activation in normal and "giant" platelets. *Blood Cells.* 9:359–382.

Frojmovic, M. M., R. M. Mooney, and T. Wong. 1993. Regulation of platelet aggregation by GPIIb-IIIa receptor expression and fibrinogen binding: platelet subpopulations responses for ADP. *Thrombos. Haemost.* 69:1002*a*. (Abstr.)

Furlan, M., J. Stiegner, and E. A. Beck. 1987. Exposure of platelet binding sites in von Willebrand factor by adsorption onto polystyrene latex particles. *Biochim. Biophys. Acta.* 429:27–37.

Gawaz, M. P., J. C. Loftus, M. L. Bajt, M. M. Frojmovic, E. F. Plow, and E. F. Ginsberg. 1991. Ligand bridging mediates integrin $\alpha_{II}\beta_3$ (platelet GPIIb-IIIa) dependent homotypic and heterotypic cell-cell interactions. *J. Clin. Invest.* 10:1128–1134.

Goldsmith, H. L., M. M. Frojmovic, S. Braovac, F. McIntosh, and T. Wong. 1994. Adenosine diphosphate-induced aggregation of human platelets in flow through tubes. III. Contributions of extrinsic fibrinogen and fibrinogen-independent flow effects. *Thromb. Haemost.* 71:78–90.

Hantgan, R. R. 1985. A study of the kinetics and mechanism of ADP-triggered platelet aggregation. *Biochim. Biophys. Acta.* 846:64–75.

Hawiger, J., M. Kloczewiak, M. A. Bednarek, and S. Timmons. 1989. Platelet receptor recognition domains on the α chain of human fibrinogen: structure-function analysis. *Biochemistry.* 28:2909–2914.

Higuchi, W. I., T. Okada, and G. A. Stelter. 1963. Kinetics of rapid aggregation in suspensions (comparison of experiments with the Smoluchowski theory). *J. Pharm. Sci.* 52:49–54.

Huang, P. Y., and J. D. Hellums. 1993. Aggregation and disaggregation kinetics of human blood platelets. Part II. Shear-induced platelet aggregation. *Biophys. J.* 65:344–353.

Ikeda, Y., M. Handa, K. Kawano, T. Kamata, M. Murata, Y. Araki, H. Anbo, Y. Kawai, K. Watanabe, I. Itagaki, S. Kiyotaka, and Z. Ruggeri. 1991. The role of von Willebrand factor and fibrinogen in platelet aggregation under varying shear stress. *J. Clin. Invest.* 87:1234–1240.

Joist, J. H., E. J. Bauman, M. Speer, and S. P. Sutera. 1985. Role of platelet surface interaction in fluid shear-induced platelet aggregation. *Thromb. Haemost.* 54:109*a* (Abstr.)

Kim, S. 1986. Singularity solutions for ellipsoids in low-Reynolds-number flows: with applications to the calculation of hydrodynamic interactions in suspensions of ellipsoids. *Int. J. Multiphase Flow.* 12:469–491.

Klose, H. J., H. Rieger, and H. Schmid-Schönbein. 1975. A rheological method for the quantification of platelet aggregation (PA) in vitro and its kinetics under defined flow conditions. *Thromb. Res.* 7:261–272.

Kouns, W., D. Kirchhifer, P. Hadvary, A. Edenhofer, T. Weller, G. Pfenninger, H. R. Baumgartner, L. K. Jennings, and B. Steiner. 1992. Reversible conformational changes induced in glycoprotein IIb-IIIa by a potent and selective peptidomimetic inhibitor. *Blood.* 80:2539–2547.

Landolfi, R., R. D. Christopher, E. D. Candia, B. Rocca, and B. Bizzi. 1991. Effect of fibrinogen concentration on the velocity of platelet aggregation. *Blood.* 78:377–381.

Lee, R. G., and S. W. Kim. 1974. Adsorption of proteins onto hydrophobic polymer surfaces:adsorption isotherms and kinetics. *J. Biomed. Mater. Res.* 8:251–259.

Lumley, P., and P. P. A. Humphrey. 1981. A method for quantitating platelet aggregation and analyzing drug-receptor interactions on platelets in whole blood in vitro. *J. Pharmacol. Methods.* 6:153–166.

Marguerie, G. A., T. S. Edgington, and E. F. Plow. 1980. Interaction of fibrinogen with its platelet receptor as part of a multistep reaction in ADP-induced platelet aggregation. *J. Biol. Chem.* 255:154–161.

Milnor, W. R. 1982. Hemodynamics. Williams & Wilkins, Baltimore, MD. 53 pp.

Niewiarowski, S., E. Kornecki, A. Z. Budzynski, T. A. Morinelli, and G. P. Tuszynski. 1983. Fibrinogen interaction with platelet receptors. *Ann. N. Y. Acad. Sci.* 408:536–555.

Pedvis, L. G., T. Wong, and M. M. Frojmovic. 1988. Differential inhibition of the platelet activation sequence: shape change, micro- and macro-aggregation, by a stable prostacyclin analogue (lloprost). *Thromb. Haemost.* 59:323–328.

Peerschke, E., and M. B. Zucker. 1981. Fibrinogen receptor exposure and aggregation of human blood platelets produced by ADP and chilling. *Blood.* 57:663–670.

Peerschke, E. I. B. 1985. The platelet fibrinogen receptor. *Semi. Haematol.* 22:241–259.

Peterson, D. M., N. A. Stathopoulos, T. D. Giorgio, J. D. Hellums, and J. L. Moake. 1987. Shear-induced platelet aggregation requires von Willebrand factor and platelet membrane glycoproteins Ib and IIb-IIIa. *Blood.* 69:625–628.

Plow, E. F., A. H. Srouji, D. Meyer, G. Marguerie, and M. H. Ginsberg. 1984. Evidence that three adhesive proteins interact with a common recognition site on activated platelets. *J. Biol. Chem.* 259:5388–5391.

Plow, E. F., and G. Marguerie. 1982. Inhibition of fibrinogen binding to human platelets by the tetrapeptide glycyl-L-prolyl-L-arginyl-L-proline. *Proc. Natl. Acad. Sci. USA.* 79:3711–3715.

Plow, E. F., and G. A. Marguerie. 1980. Participation of ADP in the binding of fibrinogen to thrombin-stimulated platelets. *Blood.* 56:553–555.

Plow, E. F., and M. H. Ginsberg. 1989. Cellular Adhesion: GP IIb-IIIa as a prototypic adhesion receptor. *Prog. Haemost. Thromb.* 9:117–156.

Potanin, C. A., V. V. Verkhusha, and P. V. Vrzheshch. 1993. Coagulation of elastic particles in shear flow: application to biological cells. *J. Colloid. Interface. Sci.* 160:405–418.

Roth, G. J. 1992. Platelets and blood vessels: the adhesion event. *Immunol. Today.* 13:100–105.

Brash, J. L., and Q. M. Samak. 1978. Dynamic interactions between human albumin and polyethylene surface. *J. Colloid Interface Sci.* 65:495–504.

Shattil, S. J., J. A. Hoxie, M. C., Cunningham, and L. F. Brass. 1985. Changes in the platelet membrane glycoprotein IIb-IIIa complex during platelet activation. *J. Biol. Chem.* 260:11107–11114.

Smoluchowski, M. 1917. Versuch einer mathematischen theorie der koagulationskinetik lösungen. *Physik. Z.* 92:129–169.

Swift, D. L., and S. K. Friedlander. 1964. The coagulation of hydrosols by Brownian motion and laminar shear flow. *J. Colloid Sci.* 19:621–647.

Tang, S. S., and M. M. Frojmovic. 1977. The effects of pCO_2 and pH on platelet shape change and aggregation for human and rabbit platelet-rich plasma. *Thromb. Res.* 10:135–145.

Timmons, S., M. A. Bednarek, M. Kloczewiak, and J. Hawiger. 1989. Anti-platelet "hybrid" peptides analogous to receptor recognition domains on γ and α chains of human fibrinogen. *Biochemistry.* 28:2919–2923.

Ugarova, T. P., A. Z. Budzynski, S. J. Shatill, Z. M. Ruggeri, M. H. Ginsberg, and E. F. Plow. 1993. Conformational changes in fibrinogen elicited by its interaction with platelet membrane glycoprotein GPIIb-IIIa. *J. Biol. Chem.* 268:21080–21087.

van de Ven, T. G. M. 1989. Colloidal Hydrodynamics. Academic Press. San Diego, CA. 582 pp.

van de Ven, T. G. M., and S. G. Mason 1977. The microrheology of colloidal dispersions. VII. Orthokinetic doublet formation of spheres. *Colloid Polymer Sci.* 255:469–479.

Varennes, S., and T. G. M. van de Ven. 1988. Effects of neutral polymers on the kinetics of particle deposition. *Physicochem. Hydrodyn.* 10: 229–238.

Warkentin, T. E., M. J. Poling, and R. M. Hardisty. 1990. Measurement of fibrinogen binding to platelets in whole blood by flow cytometry: a micromethod for the detection of platelet activation. *Br. J. Haematol.* 76:387–394.

Zamarron, C., M. H. Gingsberg, and E. F. Plow. 1991. A receptor-induced binding site in fibrinogen elicited by its interaction with platelet membrane glycoprotein IIb-IIIa. *J. Biol. Chem.* 266:16193–16199.

Zeichner, G. A., and W. R. Schowalter. 1977. Use of trajectory analysis to study stability of colloidal dispersions in flow fields. *AIChE J.* 23: 243–254.